Accepted Manuscript

Spectroscopic peculiarities of $CsCaI_3:Tm^{2+}$ single crystals examined through one-photon and excited state excitation spectroscopy

Mirosław Karbowiak, Radosław Lisiecki, Piotr Solarz, Jarosław Komar, Witold Ryba-Romanowski

PII: S0925-8388(18)30059-8

DOI: 10.1016/j.jallcom.2018.01.058

Reference: JALCOM 44522

To appear in: *Journal of Alloys and Compounds*

Received Date: 24 September 2017

Revised Date: 3 January 2018

Accepted Date: 4 January 2018

Please cite this article as: Mirosł. Karbowiak, Radosł. Lisiecki, P. Solarz, Jarosł. Komar, W. Ryba-Romanowski, Spectroscopic peculiarities of $CsCaI_3:Tm^{2+}$ single crystals examined through one-photon and excited state excitation spectroscopy, *Journal of Alloys and Compounds* (2018), doi: 10.1016/j.jallcom.2018.01.058.

Spectroscopic peculiarities of $CsCaI_3:Tm^{2+}$ single crystals examined through one-photon and excited state excitation spectroscopy

Mirosław Karbowiak[1)]*, Radosław Lisiecki[2)], Piotr Solarz[2)], Jarosław Komar[2)], Witold Ryba-Romanowski[2)]

1) *Faculty of Chemistry, University of Wrocław, F. Joliot-Curie 14, 50-383 Wrocław, Poland*
2) *Institute of Low Temperature and Structure Research, Polish Academy of Sciences, Okólna 2, 50-422 Wrocław, Poland*

ABSTRACT

The $CsCaI_3$ single crystals doped with Tm^{2+} were grown by Bridgman technique. Divalent thulium luminescence related to the $4f^{13}$-$4f^{13}$ intra-configurational and $4f^{12}5d^1$-$4f^{13}$ inter-configurational transitions were analyzed as a function of temperature. Excited state excitation spectroscopy has been applied within a wide spectral range to examine peculiarities of transitions between different $4f^{12}5d^1$ excited states of Tm^{2+}. This two-color excitation experiment was useful to assess d-d photon-absorption processes that are relevant to observed up-conversion phenomena attributed to effective anti-Stokes green luminescence around 550 nm. Furthermore, activation energy of $4f^{12}5d^1 \rightarrow 4f^{13}$ luminescence quenching was estimated and high value of $^2F_{5/2} \rightarrow {}^2F_{7/2}$ emission cross-section was determined in $CsCaI_3:Tm^{2+}$. Our spectroscopic study was performed to complement and verify the previous investigation in this field.

Keywords:
Rare earth alloys and compounds
Optical absorption spectroscopy
Divalent thulium
$CsCaI_3$
Excited state excitation

1. Introduction

In recent years there has been a steady increase in the theoretical and experimental studies of divalent lanthanide ions (Ln^{2+}) doped in inorganic materials. Although the most abundant data exist for divalent samarium, europium and ytterbium, which are most easily reducible from the trivalent to divalent state [1], interconfigurational $4f^N$ - $4f^{N-1}5d^1$ transitions of other Ln^{2+} ions have also received appreciable attention owing to their technological applications [2]. The intense and broad emission of divalent europium is desirable in phosphors [3,4,5,6]. The Sm^{2+}-doped materials are found as effective light conversion optical systems [7,8] and highly sensitive optical temperature sensors [9]. The Tm^{2+} doped halides exhibit promising properties for applications as efficient luminescent solar concentrators [10], whereas SrB_4O_7 host activated with divalent thulium ions can be considered as a potential laser material and optical temperature sensor [11]. Possible laser applications were recognized for $4f^{12}5d^1$-$4f^{13}$ transitions of Yb^{2+} [12]. It is well known that the critical issue for stabilization of lanthanide ions in their divalent state is the choice of appropriate host matrix [13]. In this regard a ternary halides $CsCaX_3$ (X = Cl, Br or I) that crystallize in a perovskite structure and belong to orthorhombic crystalline system with Ca^{2+} ions in the distorted octahedral coordination appear as very suitable hosts for stabilization of divalent lanthanides. $CsCaX_3$ crystals contain divalent sites, hence the Ln^{2+} ions can be conveniently incorporated into host lattice. Several papers have been devoted to investigation of spectroscopic properties of divalent lanthanide ions in halidoperovskites. The spectroscopic properties of Eu^{2+} ions doped in the perovskites CsCaX3 and CsSrX3 (X = Cl, Br, and I), which are considered as novel promising scintillators [14,15,16], were studied in [17]. The same compounds doped with Yb^{2+} ions also exhibit properties suitable for their applications in high-energy detection devices [18]. The comparative studies of photoluminescence properties of Yb^{2+} ions doped in the halidoperovskites $CsMX_3$ (M = Ca, Sr; X = Cl, Br, I) were presented [19] followed by systematic studies of the decay times and temperature dependence of the spin-enabled and spin-forbidden transitions of Yb^{2+} ions in these hosts [18, 20].

Halidoperovskites doped with Tm^{2+} ions appear as particularly interesting systems since different types of light emission were recognized in Tm^{2+}-doped $CsCaCl_3$, $CsCaBr_3$ and $CsCaI_3$ crystals. The occurrence of multiple emitting $4f^{12}5d^1$ states in Tm^{2+} was recently explained by

using *ab initio* calculations [21]. Radiative and nonradiative relaxation processes were studied and discussed for these systems [22,23,24]. The same authors reported on detailed analysis of Tm-doped halide crystals absorption spectra in the region of 4f-4f and 4f-5d excitations [25]. It has been shown that Tm^{2+} ions offer excellent advantage for the study of 4f-5d excitation processes. In subsequent studies the upconversion (UC) phenomena have been observed in $CsCaI_3:Tm^{2+}$ crystals under excitation at 810 nm [26,27]. It is unusual type of upconversion phenomena involving the 4f-5d states of Tm^{2+}. Understanding of $4f^{12}5d^1$ excited states are highly essential to explore peculiarities of multiple emission and UC processes in materials doped with divalent thulium ions. It has been recently proved that two-photon experiment is an useful method to characterize lanthanide excited states including transitions between different $4f^{N-1}5d^1$ multiplets [28]. In particular it is especially suitable for probing the equilibrium distance offset between different $4f^n - 4f^{n-1}5d^1$ excited states [28,29] Since for Tm^{2+} in $CsCaI_3$ emission originates not only from the lowest but also from the higher $4f^{12}5d^1$ excited state it is a very suitable system for two-photon excited state excitation spectroscopy (ESE). UC process involving exclusively $4f^{12}5d^1$ excited states has already been demonstrated in $CsCaI_3:Tm^{2+}$ system [26,27], but only using excitation at a single wavenumber. The ESE experiment has not been reported.

The main aim of this study is to gain deeper insights into processes behind UC involving $4f^{12}5d^1$ excited states of Tm^{2+} ion in $CsCaI_3$. Accordingly, in this work one photon excitation spectroscopy and especially two-photon excited state excitation spectroscopy (ESE) are employed to investigate and analyze $4f^{13}$ and $4f^{12}5d^1$ states responsible for activation of the observed down-converted and up-converted Tm^{2+} luminescence. A significant decrease of the $4f^{12}5d^1 \rightarrow 4f^{13}$ luminescence lifetime was observed above T = 190 K and effective value of $^2F_{5/2} \rightarrow {}^2F_{7/2}$ emission cross-section was estimated for $CsCaI_3:Tm^{2+}$ crystal. Our original results are discussed in relation to previously obtained data for Tm^{2+} in $CsCaI_3$. Moreover, the noticeable differences between spectroscopic properties of investigated divalent thulium doped iodide crystal and those reported for $CsCaCl_3:Tm^{2+}$ and $CsCaBr_3:Tm^{2+}$ are observed and discussed.

2. Experimental section

$CsCaI_3$ single crystals doped with 0.14 at.% and 0.68 at.% of Tm^{2+} (as determined with ICP-OES spectroscopy) were grown by Bridgman technique. Pure $CsCaI_3$ single crystal, prepared from stoichiometric amounts of CsI and CaI_2, was crushed and mixed with appropriate amount of TmI_2, then placed in a vitreous carbon crucible, which was put into silica ampoule and heated for several hours at 720 K under high dynamic vacuum. After sealing under vacuum the ampoule was lowered through the vertical furnace at 1015 K at a rate of 5 mm/h. TmI_2 used in this procedure was earlier synthesized via metallothermic route [30] in reaction of anhydrous TmI_3 with Tm powder (99.9%, Sigma-Aldrich) at 1125 K in a sealed niobium tube. TmI_3 was prepared from Tm_2O_3 (99.99%, Stanford Materials) by the ammonium halide route [31]. The obtained crystals were of good optical quality (Fig. S1). The crystals were cut and polished in the argon glove-box and placed in airtight copper cuvette with quartz windows for absorption measurements or sealed in a quartz tube under low-pressure of helium gas for emission measurements.

The emission spectra were excited by a MDL-N-808-10W diode laser at 808 nm and MXL-F-445-3W diode laser at 445 nm, respectively. The luminescence was dispersed by an Optron Dongwoo monochromator with 750 mm focal length and detected by a Hamamatsu R955 photomultiplier or InGaAs detector depending on the spectral range. The excitation spectrum was recorded with a Dongwoo Model Scanning System consisting of LPS-200X Xenon Lamp, an excitation monochromator with 150 mm focal length, an emission monochromator having 750 mm focal length and a Hamamatsu R955 photomultiplier. Excited State Excitation spectra were recorded using MDL-N-808-10W diode laser as first excitation source. Up-converted green luminescence was monitored on Dongwoo DM711 monochromator and detected by a Hamamatsu R3896 photomultiplier. The second excitation pulses fluently tuned in the required spectral regions were delivered from Opotek Opolette 355 LD laser system. To record luminescence decay curves a femtosecond laser (Coherent Model ‘‘Libra’’) that delivers a train of 89 fs pulses at a centre wavelength of 800 nm and a pulse energy of 1 mJ with a repetition rate regulated up to 1 kHz was used as an excitation source. To obtain light pulses at different wavelengths (230-2800 nm) the laser is coupled to an optical parametric amplifier (Light Conversion Model ‘‘OPerA’’). Luminescence decay curves were recorded with a grating spectrograph (Princeton Instr. Model Acton 2500i) coupled to a streak camera (Hamamatsu Model C5680). For spectroscopic measurement at low temperature the samples were placed in an

Oxford Model CF 1204 continuous flow liquid helium cryostat equipped with a temperature controller.

3. Results and discussion

$CsCaI_3$ crystallizes in the orthorhombic Pbnm space group [32] and in dopped crystals Tm^{2+} ions substitute for Ca^{2+} ions on a slightly distorted octahedral site (the actual site symmetry for Tm^{2+} ions is C_1).

Fig. 1 reveals the excitation spectrum of $CsCaI_3$:0.14% Tm^{2+} visible luminescence monitored at 547 nm and measured at T = 5K within 250 - 540 nm spectral region. The excitation spectrum is quite complex and consists of numerous broad bands, while some of them exhibit additional fine structure. The bands observed in the spectrum are due to transitions from the ground $^2F_{7/2}$ multiplet of the $4f^{13}$ configuration to the states of the $4f^{12}5d^1$ configuration [33]. Octahedral ligand-field interaction in $CsCaI_3$:Tm^{2+} results in splitting of 5d orbitals into t_{2g} and e_g sets of levels. These levels are coupled to $^{2S+1}L_J$ multiplets of $4f^{12}$ core originating from spin-orbit and Coulomb interactions. The resulting states will be labeled as ($^{2S+1}L_J$, t_{2g}) and ($^{2S+1}L_J$, e_g), respectively. The Coulomb interactions between the 5d electron and the $4f^{12}$ core electrons additionally split these states into high-spin (S = 3/2) and low-spin (S = 1/2) states. The energy-level diagram of Tm^{2+} in $CsCaI_3$ as well as the radiative and nonradiative processes relevant to the discussion presented in this study are shown in the inset in Fig. 1.

According to energy level diagram in Fig. 1 the first intense band observed in the excitation spectrum with maximum at ~19375 cm^{-1} (516 nm) should be assigned to $^2F_{7/2} \rightarrow (^3F_4, t_{2g})$ transitions, whereas the group of bands observed in the 20500 - 25000 cm^{-1} range, with maxima at about 21680 cm^{-1} (461 nm), 22730 cm^{-1} (440 nm) and 23830 cm^{-1} (420 nm) are attributed to $^2F_{7/2} \rightarrow (^3H_6, e_g)$ transitions.

Near-infrared emission spectrum of Tm^{2+} was acquired in 1100-1200 nm spectral range after excitation of $CsCaI_3$:0.68% Tm^{2+} crystal at 445 nm. Fig. 2 (a) compares luminescence spectra of Tm^{2+} in the near-infrared region measured at several different temperatures between 5 and 300 K. The spin-orbit interaction splits the ^2F term of the ground $4f^{13}$ configuration of Tm^{2+} into the ground $^2F_{7/2}$ and the excited $^2F_{5/2}$ multiplet. Accordingly, the observed emission band is related to f-f intra-configurational $^2F_{5/2} \rightarrow {}^2F_{7/2}$ transitions of Tm^{2+}. It can be discerned that influence of temperature on the infrared luminescence excited at 445 nm in $CsCaI_3$:0.68% Tm^{2+}

is significant. Integrated luminescence intensity for the spectrum measured at T = 300 K is smaller by a factor of six as compared to that recorded at T = 200 K. In the room-temperature NIR emission spectrum of Tm^{2+} one pronounced peak with maximum at 8767 cm^{-1} is observed and its FWHM value was determined to be 144 cm^{-1}. The Füchtbauer-Ladenburg method was used to estimate the emission cross-section. The dependence between the emission cross-section σ_{em} and emission spectrum is described as:

$$\sigma_{em}(\lambda) = \frac{\beta \lambda^5 I(\lambda)}{8\pi n^2 c \tau_{rad} \int \lambda I(\lambda) d\lambda} \quad (1)$$

where $I(\lambda)$ represents the experimental emission intensity at the wavelength λ, c is the light velocity, n, β and τ_{rad} are the refractive index of material, branching ratio and radiative lifetime of the $^2F_{5/2}$ multiplet, respectively. It was assumed that luminescence lifetime of 0.65 ms measured for diluted sample is not significantly different than $^2F_{5/2}$ radiative lifetime. Inset of Fig. 2 presents simulated emission cross-section spectrum derived from the $^2F_{5/2} \rightarrow {}^2F_{7/2}$ luminescence of Tm^{2+} excited at 445 nm. The prominent line at 1141 nm dominates emission cross-section spectrum with advantageously high peak value which amounts to σ_{em} = 6.07 x 10^{-20} cm^2. For a comparison, significantly lower value of emission cross section σ_{em} = 3.50 x 10^{-20} cm^2 was found for SrB_4O_7:Tm^{2+} [34].

Fig. 2 (b) presents the Tm^{2+} NIR emission spectrum measured at T = 5 K. At this temperature only the lowest-energy crystal field sublevel of the emitting state is substantially populated and four emission lines are expected for $^2F_{5/2} \rightarrow {}^2F_{7/2}$ transitions having in mind that divalent thulium ions are coordinated by six I^- ligands in a distorted octahedral sites of C_1 symmetry in $CsCaI_3$ lattice. In accordance with this expectation the emission spectrum presented in Fig. 2 is dominated by four sharp lines located at 8634, 8721, 8773 and 8854 cm^{-1}. It should be mentioned that only two $^2F_{5/2} \rightarrow {}^2F_{7/2}$ emission lines identified at 8782 cm^{-1} and 8790 cm^{-1} by J. Grimm et al. [22], were assigned by these authors as electronic transitions. The remaining emission lines placed at longer wavelengths were found as vibronic sidebands. In a short-wavelength part of our spectrum the additional structureless band appears at 8140 cm^{-1}. In view of a fast decay of this emission ($\tau \approx 1$ μs) it may be associated with transitions between levels of initial ($^3F_4$,t_{2g}) and terminal ($^3H_4$,t_{2g}) manifolds. The decay curves of observed luminescence are presented in Fig. 2 (c,d). The 10 Dq crystal-field splitting of the 5d part of the $4f^{12}5d^1$

electron configuration in $CsCaI_3:Tm^{2+}$ was estimated to be 8500 cm^{-1} and more than fifteen cut-off phonons are needed to bridge the ($^3F_4$,t_{2g}) - ($^3H_4$,t_{2g}) energy gap. It is quite enough for ($^3F_4$,t_{2g}) components to become emissive levels and consequently, the excitation energy may be down-converted to obtain NIR photons as result of d-d transitions.

Aside from f-f NIR emission of Tm^{2+} the visible luminescence of $CsCaI_3$:0. 68% Tm^{2+} crystal was detected at T = 5 K upon excitation at 445 nm and 808 nm as it is displayed in the Fig. 3. In fact, these spectra consist of one prominent structureless emission band centered in green spectral region at 547 nm. When the ($^3F_4$, t_{2g}) Tm^{2+} multiplet is excited at λ = 445 nm down-converted emission occurs. The energy gap between the ($^3F_4$,t_{2g}) $\leftrightarrow$ ($^3H_6$,t_{2g}) multiplets was found to be 2700 cm^{-1} whereas a maximum energy of phonons in $CsCaI_3$ is $\hbar\omega_{max.}$= 170 cm^{-1} [14]. Accordingly, efficient radiative transitions from the ($^3F_4$, t_{2g}) multiplet take place. The green Tm^{2+} emission is associated with a transition from the lowest excited state of the ($^3F_4$, t_{2g}) multiplet to the $^2F_{7/2}$ Tm^{2+} ground state. The inset in Fig. 3 presents the magnified fragment of emission spectrum recorded in 11500-13500 cm^{-1} range when excited at 445 nm. This emission band peaked at 12100 cm^{-1} is associated with ($^3H_6$, t_{2g}) $\rightarrow$ $^2F_{7/2}$ transitions.

When the $CsCaI_3$:0.68% Tm^{2+} crystal is excited at 808 nm the up-converted luminescence is found (Fig. 3). In this case the ($^3H_6$, t_{2g}) S = 3/2 multiplet is excited as a result of the spin-forbidden transitions. The observed upconversion phenomena is atypical because the adequate $4f^{12}5d^1$ Tm^{2+} excited states are involved to populate the divalent thulium luminescent levels. Efficiency of the green up-converted emission in $CsCaI_3$:0.68% Tm^{2+} is relatively high. The up-converted emission with a maximum located at λ = 546 nm when excited at 12350 cm^{-1} (809.7 nm) has been reported by J. Grimm et. al. [24,27]. In contrast to the Tm^{2+} luminescence presented in [24] our emission spectrum is characterized by a more intense band located at 485 nm (20618 cm^{-1}) that can be attributed to transitions originating in the higher-energy levels of ($^3F_4$, t_{2g}) multiplet. It has been concluded that two-photon excitation process is responsible for population of Tm^{2+} luminescent level in upconversion phenomena. Furthermore it has been assumed that the Tm^{2+} up-converted luminescence in $CsCaI_3$ mainly results from GSA (Ground State Absorption) /ESA (Excited State Absorption) process but contribution of GSA/ETU (Energy Transfer Upconversion) process is considered as well [27]. Upconversion phenomena in Tm^{2+}-doped iodide can be effective because excited state absorption and energy transfer

upconversion processes involve $5d(t_{2g}) \rightarrow 5d(e_g)$ excitation transitions [26] which are characterized by quite high values of oscillator strength.

Up-conversion phenomena observed in $CsCaI_3:Tm^{2+}$ are activated by transitions between $4f^{12}5d^1$ excited states. In order to get more detailed insight into these transitions a two-color excitation experiment was performed. The set-up consisting of two laser sources, namely a CW AlGaAs- diode laser and a tunable pulsed OPO laser was used to record excitation spectra in wide spectral regions. When CW λ = 808 nm excitation wavelength is employed, a ground-state absorption occurs and the ($^3H_6$, t_{2g}) multiplet is continuously populated. An additional pulsed excitation at varied wavelengths stimulate the already excited Tm^{2+} ions to populate the higher energy $4f^{12}5d^1$ states. A second photon is resonant with the energy separation between involved Tm^{2+} excited states. Eventually, excited state excitation spectra of $CsCaI_3$:0.68% Tm^{2+} monitoring anti-Stokes green emission at 547 nm were measured and are presented in Fig. 4. When the combination of these both aforementioned excitation sources was used the green UC emission signal was certainly enhanced comparing to CW single – laser excitation. This may indicate that ESA ($^3H_6$, t_{2g}) $\rightarrow$ ($^3F_4$, t_{2g}) contribution in UC process is highly relevant in $CsCaI_3:Tm^{2+}$ crystal.

Two-color excited state excitation experiment can be utilized to examine equilibrium distance offset the involved $4f^{12}5d^1$ states. It was assumed that electronic transitions between two excited states with comparable equilibrium bond lengths are related to ESE sharp spectral line while transitions between contracted and expanded excited states give rise to broad bands [28]. Our excited state excitation spectrum displayed in Fig. 4 consists of a few broad bands (labeled A-D) placed within 6830-8330 cm^{-1}, 8665-9340 cm^{-1}, 11095-13825 cm^{-1} and 14100- 16815 cm^{-1} spectral ranges. The lower-energy ESE (A-B) bands can be attributed to ($^3H_6$, t_{2g}) $\rightarrow$ ($^3F_4$, t_{2g}) transitions and the remaining broadened bands (C-D) located at higher energy may be associated with two-photon absorption transitions to $4f^{12}5d(t_{2g}/e_g)^1$ mixed states. At lower energy sides of A and B ESE bands sharp and narrow lines can be discerned, which begin to appear at 6987 cm^{-1} and 8766 cm^{-1}, respectively. These sharp components are related to transitions characterized by no change in potential energy surfaces equilibrium position of the various $4f^{12}5d(t_{2g})^1$ excited states. In accordance with that for low-energy f-d states of Tm^{2+} in $CsCaI_3$ there is rather similar Tm-ligand equilibrium distance in their potential energy surface. The adequate set of ESE bands attained during a two-photon excitation experiment was recently observed by M. de Jong. et. al.

[28] for $CsCaCl_3:Tm^{2+}$ and $CsCaBr_3:Tm^{2+}$ crystals. The onset of two observed groups of lines has been then established at 7100 cm^{-1} and 9000 cm^{-1}. It means that ($^3H_6$, t_{2g}) → ($^3F_4$, t_{2g}) ESE bands observed for $CsCaI_3:Tm^{2+}$ are slightly shifted toward lower energy in relation to the chloride and bromide counterparts. It stems from more covalent character of iodide host as compared to chloride or bromide hosts as well as from differences in a crystal-field strength. Both these factors exert strong effect on barycenter of $4f^{12}5d^1$ configuration and energies of d-d transitions. The ESE band measured for $CsCaI_3:Tm^{2+}$ contain more narrow and sharp lines than it is observed in $CsCaCl_3:Tm^{2+}$. This finding may be a consequence of a higher site symmetry of Tm^{2+} ion in chloride (C_{4h}) than in iodide (C_1) crystal. As compared to previous results [28] our excited state excitation experiment was performed using higher-energy second excitation photons and ESE spectra were acquired up to 16800 cm^{-1}. Actually, above 11000 cm^{-1} broad and structureless bands appear, centered at 12037, 13492, 14804 and 15782 cm^{-1}. These intense ESE bands may correspond to two-photon absorption from ($^3H_6$, t_{2g}) state to higher-energy $4f^{12}5d^1$ states. The high intensity of ESE bands results from a large value of d-d two-photon absorption cross-section [35]. The spectral character of these broad bands implies that larger difference between equilibrium distance in potential energy surface of lower- and higher-energy $4f^{12}5d^1$ states occurs in $CsCaI_3:Tm^{2+}$.

Fig. 5 displays results of an experiment assessing the impact of temperature on thulium excited state relaxation dynamics. The visible luminescence decay curves were measured in a region 5 – 300 K at $\lambda_{det.}$=547 nm under femtosecond pulse excitation at $\lambda_{exc.}$= 450 nm. The relaxation of f-d ($^3F_4$, t_{2g}) states in $CsCaI_3:Tm^{2+}$ may result from radiative transitions and nonradiative multiphonon transitions. The energy separation between ($^3F_4$, t_{2g}) and ($^3H_6$, t_{2g}) states of Tm^{2+} was found to be 2700 cm^{-1} and roughly sixteen cut-off phonons are needed to bridge this energy gap. Accordingly, in this case the nonradiative relaxation should be effectively suppressed. Estimated experimental lifetime of green Tm^{2+} emission ($\tau \approx 1.3$ μs) is practically constant from T = 5 K up to 190 K. Subsequently, at the higher temperature the lifetime is significantly shortened and amounts to 7 ns at room temperature. It is worth noticing that a single exponential time dependence was recognized for all analyzed decay curves. The luminescence decay curves measured at T=5K, 77 K and 298 K are presented in a lower part of Fig 5. The exponential decay function $I=I_0+Aexp(-t/\tau_{exp.})$ was used to determine the adequate experimental lifetimes.

Effect of thermal energy on Tm^{2+} transition rates has been assessed with the Arrhenius plots defined as

$$W = A\exp\left(\frac{-E_q}{kT}\right) \quad (2)$$

equation (1) can be transformed to

$$\ln(W) = \ln(A) - \frac{E_q}{kT} \quad (3)$$

where W is the transition rate and A (s^{-1}) denotes a transition rate given by the intercept of the line at $1/T \rightarrow 0$ and is attributed to pre-exponential factor, k is Boltzmann constant and T is temperature. The parameter E_q (quenching energy, (cm^{-1})) is obtained from the fit of the (2) line. The lowest energy states of the $4f^{12}5d^1$ Tm^{2+} configuration are thermally populated with temperature increasing and dynamics of $4f^{12}5d^1$-$4f^{13}$ vibronic transitions is more effective. Consequently, an increase of relaxation rate is observed as it is presented in inset of Fig. 5. The activation energy was estimated to be 2697±15 cm^{-1}. It means that our finding is highly consistent with the reported $\Delta E = 2700$ cm^{-1} for energy gap between ($^3F_4$, t_{2g}) and ($^3H_6$, t_{2g}) states in $CsCaI_3$:Tm^{2+}. The comparable experimental lifetime of 1 μs at T = 10 K was determined for $CsCaI_3$:1 at.% Tm^{2+} by J. Grimm et. al. [24]. Furthermore, these authors have observed that green radiative transitions are effective up to about 250 K and above this temperature the up-converted emission rapidly drops. This finding is consistent with our results revealing substantial decrease of measured lifetime already around T=200 K. It was documented that radiative rate constant R of ($^3F_4$, t_{2g}) $\rightarrow$ $^2F_{7/2}$ emission is the most prominent relaxation path in the iodide up to 220 K. Above this temperature nonradiative relaxation to ($^3H_6$, t_{2g}) state is a dominant process [24]. It is worth noticing that the presented spectroscopic results for $CsCaI_3$:0.68% Tm^{2+} crystal are comparable to those obtained for $CsCaI_3$:0.14% Tm^{2+}, hence no significant differences were found for the sample containing lower divalent thulium concentration.

4. Conclusions

The spectroscopic properties of Tm^{2+} - doped $CsCaI_3$ single crystals were investigated in relation to previously reported data. Novel and valuable results were achieved particularly pertinent to excited state excitation experiment performed in a wide spectral range. Acquired excited excitation spectra are useful for analysis of d-d photon-absorption processes relevant especially in observed up-conversion phenomena. The $4f^{12}5d \rightarrow 4f^{13}$ luminescence was analyzed as a function of temperature. The calculated activation energy was found to be fully in compliance to $(^3F_4, t_{2g}) \leftrightarrow (^3H_6, t_{2g})$ excited states energy gap. Moreover Füchtbauer–Ladenburg method was applied to estimate high value of emission cross section for NIR $^2F_{5/2} \rightarrow {}^2F_{7/2}$ transition in $CsCaI_3$:0.68% Tm^{2+}. The noticeable differences between spectroscopic properties of investigated divalent thulium doped iodide crystal and those reported for $CsCaCl_3:Tm^{2+}$ and $CsCaBr_3:Tm^{2+}$ can be underlined. Emission bands measured for $CsCaI_3:Tm^{2+}$ are located at lower energies in relation to chloride and bromide counterparts. We observed that the $^2F_{5/2} \rightarrow {}^2F_{7/2}$ emission intensity decreases significantly at T=250 K in $CsCaI_3:Tm^{2+}$ whereas this efficient quenching process occurs at T=100 K for $CsCaCl_3:Tm^{2+}$ and at T=150 K for $CsCaCl_3:Tm^{2+}$. The green up-converted emission is observed for all halides but this luminescence is especially efficient in $CsCaI_3:Tm^{2+}$ since a large $(^3F_4, t_{2g})$ - $(^3H_6, t_{2g})$ energy gap is high enough for effective radiative transitions. Our excited state excitation experiment reveals some differences in the (ESE) spectra measured for iodide crystals and these studied for chloride and bromide. ESE bands related to different excited $4f^{12}5d^1$ states in $CsCaI_3:Tm^{2+}$ are shifted toward lower energy as compared to those recorded for chloride and bromide counterparts. These variations in energy level structure of the f–d states in Tm^{2+}-doped halides are relevant for efficiency of processes involved in upconversion phenomena as well.

Appendix A. Supplementary data

Supplementary data related to this article can be found at ...

Acknowledgment

The National Science Centre (Poland) supported this work under research project DEC-2012/07/B/ST4/00581.

References

[1] G. Meyer, The divalent state in solid rare earth metal halides, in: The rare earth elements, ed. D. A. Atwood, John Wiley & Sons, 2012

[2] X. Qin, X. Liu, W. Huang, M. Bettinelli, X. Liu, Lanthanide-activated phosphors based on 4f-5d Optical transitions: Theoretical and experimental aspects, Chem. Rev. 117 (2017) 4488−4527.

[3] B. Budde, H. Luo, P. Dorenbos, E. van der Kolk, Luminescent properties and energy level structure of CaZnOS:Eu^{2+}, Opt. Mater. 69 (2017) 378–381.

[4] K. Fiaczyk, E. Zych, On peculiarities of Eu^{3+} and Eu^{2+} luminescence in Sr_2GeO_4 host, RSC Adv. 6 (2016) 91836–91845.

[5] J. Ueda, T. Shinoda, S. Tanabe, Evidence of three different Eu^{2+} sites and their luminescence quenching processes in $CaAl_2O_4$:Eu^{2+}, Opt. Mater. 41 (2015) 84–89.

[6] K. Lemański, W. Walerczyk, P.J. Dereń, Luminescent properties of europium ions in $CaAl_2SiO_6$, J. Alloys Compd. 672 (2016) 595–599.

[7] J. Sun, J. Zhu, X. Liu, H. Du, Luminescence properties of SrB_4O_7:Sm^{2+} for light conversion agent, J. Rare Earths. 30 (2012) 1084–1087.

[8] P. Solarz, M. Karbowiak, M. Głowacki, M. Berkowski, R. Diduszko, W. Ryba-Romanowski, Optical spectra and crystal field calculation for SrB_4O_7:Sm^{2+}, J. Alloys Compd. 661 (2016) 419–427.

[9] Z. Cao, X. Wei, L. Zhao, Y. Chen, M. Yin, Investigation of SrB_4O_7:Sm^{2+} as a multimode temperature sensor with high sensitivity, ACS Appl. Mater. Interfaces 8 (2016) 34546−34551.

[10] O. M. ten Kate, K. W. Krämer, E. van der Kolk, Efficient luminescent solar concentrators based on self-absorption free, Tm^{2+} doped halides, Sol. Energy Mater. Sol. Cells 140 (2015) 115–120.

[11] P. Solarz, J. Komar, M. Głowacki, M. Berkowski, W. Ryba-Romanowski, Spectroscopic characterization of SrB_4O_7:Tm^{2+}, a potential laser material and optical temperature sensor, RSC Adv. 7 (2017) 21085–21092.

[12] P.S. Senanayake, J.P.R. Wells, M.F. Reid, R.B. Hughes-Currie, G. Berden, R.J. Reeves, A. Meijerink, Temporal dynamics of the frequency non-degenerate transient photoluminescence enhancement observed following excitation of inter-configurational f→d transitions in CaF_2:Yb^{2+}, J. Lumin. 192 (2017) 608–615.

[13] J. Grimm, O.S. Wenger, K.W. Krämer, H.U. Güdel, 4f-4f and 4f-5d excited states and luminescence properties of Tm^{2+}-doped CaF_2, $CaCl_2$, $SrCl_2$ and $BaCl_2$, J. Lumin. 126 (2007) 590-596.

[14] N.V. Rebrova, A. Yu. Grippa, T.E. Gorbacheva, V. Yu. Pedash, S.U. Khabuseva, V.L. Cherginets, A.N. Puzan, V.A. Tarasov, Scintillation properties of Eu^{2+}-activated $CsCaCl_{3-x}Br_x$ (x=1, 1.5, 2), J. Lumin. 182 (2017) 172-176.

[15] N.V. Rebrova, A. Yu. Grippa, A.S. Pushak, T.E. Gorbacheva, V. Yu. Pedash, V.A. Tarasov, V.L. Cherginets, Scintillation properties of crystals based on ternary bromides of calcium and alkali metals activated with europium, Cryst. Res. Technol. 52 (2017) 1600404.

[16] M. Loyd, A. Lindsey, M. Patel, M. Koschan, C.L. Melcher, M. Zhuravleva, Crystal structure and thermal expansion of $CsCaI_3$:Eu and $CsSrBr_3$:Eu scintillators, J. Cryst. Growth 481 (2018) 35–39.

[17] M. Suta, C. Wickleder, Photoluminescence of $CsMI_3$:Eu^{2+} (M = Mg, Ca, and Sr) - a spectroscopic probe on structural distortions, J. Mater. Chem. C 3 (2015) 5233-5245.

[18] M. Suta, C. Wickleder, Spin Crossover of Yb^{2+} in $CsCaX_3$ and $CsSrX_3$ (X = Cl, Br, I) – A Guideline to novel halide-based scintillators, Adv. Funct. Mater. 27 (2017) 1602783.

[19] M. Suta, W. Urland, C. Daulb C. Wickleder, Photoluminescence properties of Yb^{2+} ions doped in the perovskites CsCaX3 and CsSrX3 (X = Cl, Br, and I) – a comparative study, Phys. Chem. Chem. Phys.,18 (2016) 13196-13208.

[20] M. Suta, T. Senden, J. Olchowka, M. Adlung, A. Meijerink, C. Wickleder, Decay times of the spin-forbidden and spin-enabled transitions of Yb^{2+} doped in $CsCaX_3$ and $CsSrX_3$ (X = Cl, Br, I), Phys.Chem.Chem.Phys. 19 (2017) 7188-7194.

[21] M. de Jong, A. Meijerink, L. Seijo, Z. Barandiarán, Energy level structure and multiple $4f^{12}5d^1$ emission bands for Tm^{2+} in halide perovskites: theory and experiment, J. Phys. Chem. C 121 (2017) 10095−10101.

[22] J. Grimm, H.U. Güdel, Five different types of spontaneous emission simultaneously observed in Tm^{2+} doped $CsCaBr_3$, Chem. Phys. Lett. 404 (2005) 40–43.

[23] J. Grimm, J.F. Suyver, E. Beurer, G. Carver, H.U. Gudel, Light-Emission and Excited-State Dynamics in Tm^{2+} Doped $CsCaCl_3$, $CsCaBr_3$, and $CsCaI_3$, J. Chem. Phys. 110 (2006) 2093–2101.

[24] E. Beurer, J. Grimm, P. Gerner, H.U. Güdel, Absorption, light emission, and upconversion properties of Tm^{2+} -doped $CsCaI_3$ and $RbCaI_3$, Inorg. Chem. 45 (2006) 9901–9906.
[25] J. Grimm, E. Beurer, H.U. Güdel, Crystal absorption spectra in the region of 4f-4f and 4f-5d excitations in Tm^{2+} -doped $CsCaCl_3$, $CsCaBr_3$, and $CsCaI_3$, Inorg. Chem. 45 (2006) 10905–10908.
[26] E. Beurer, J. Grimm, P. Gerner, H.U. Güdel, New type of near-infrared to visible photon upconversion in Tm^{2+}-doped $CsCaI_3$, J. Am. Chem. Soc. 128 (2006) 3110–3111.
[27] J. Grimm, E. Beurer, P. Gerner, H.U. Güdel, Upconversion between 4f-5d excited states in Tm^{2+}-doped $CsCaCl_3$, $CsCaBr_3$, and $CsCaI_3$, Chem. Eur. J. 13 (2007) 1152–1157.
[28] M. de Jong, D. Biner, K.W. Krämer, Z. Barandiarán, L. Seijo, A. Meijerink, New Insights in $4f^{12}5d^1$ Excited States of Tm^{2+} through Excited State Excitation Spectroscopy, J. Phys. Chem. Lett. 7 (2016) 2730–2734.
[29] M.F. Reid, L. Hu, S. Frank, C.-K. Duan, S. Xia, M. Yin, Spectroscopy of high-energy states of lanthanide ions. Eur. J. Inorg. Chem. (2010) 2649-2654.
[30] G. Meyer, L.R. Morss, eds., Synthesis of Lanthanide and Actinide Compounds, Springer Netherlands, Dordrecht, 1991.
[31] G. Meyer, E. Garcia, J.D. Corbett, The Ammonium Chloride Route to Anhydrous Rare Earth Chlorides—The Example of YCl_3, in: H.R. Allcock (Ed.), Inorg. Synth., John Wiley & Sons, Hoboken, NJ, USA, n.d.: pp. 146–150.
[32] G. Schilling, G. Meyer, Z. Anorg. Allg. Chem. 622 (1996) 759-765.
[33] B. Henderson, G. Imbusch, Optical Spectroscopy of Inorganic Solids, (1989).
[34] P. Solarz, J. Komar, M. Głowacki, M. Berkowski, W. Ryba-Romanowski, Spectroscopic characterization of SrB_4O_7 :Tm^{2+} , a potential laser material and optical temperature sensor, RSC Adv. 7 (2017) 21085–21092.
[35] C.J. Dalzell, T.P.J. Han, I.S. Ruddock, The two-photon absorption spectrum of ruby and its role in distributed optical fibre sensing, Appl. Phys. B Lasers Opt. 103 (2011) 113–116.

Figures

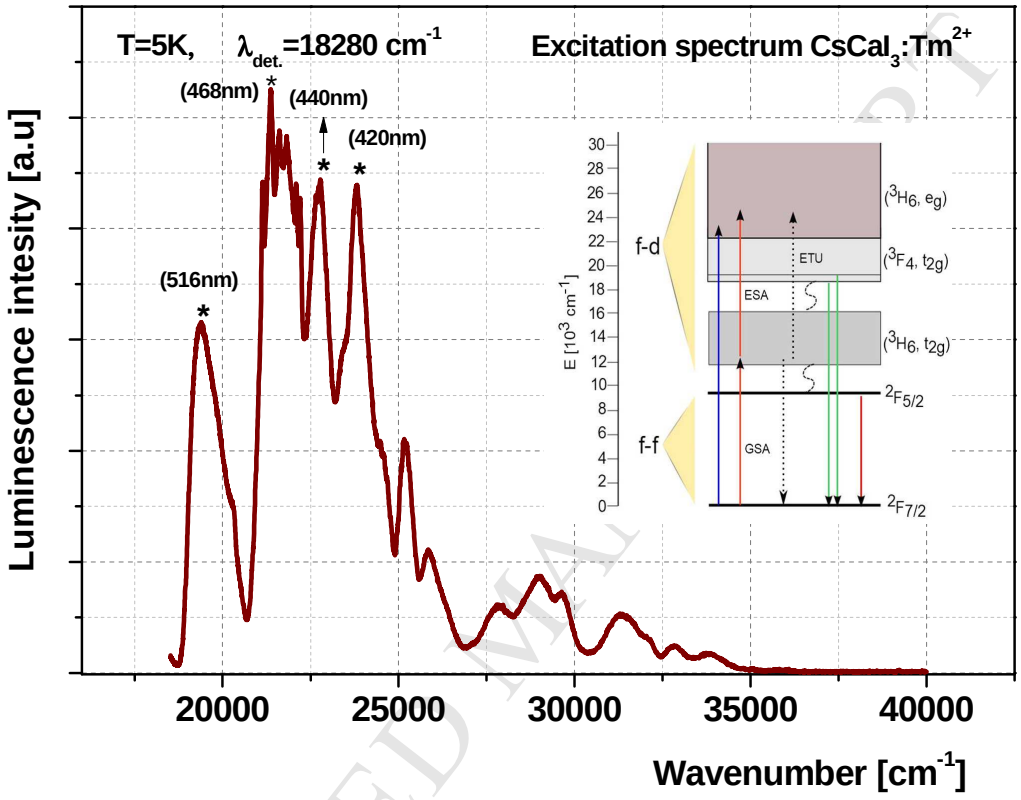

Fig. 1 One-photon excitation spectrum of $CsCaI_3$:0.68% Tm^{2+} recorded at 5 K while monitoring emission at λ = 547 nm. Inset presents energy-level diagram of Tm^{2+} in $CsCaI_3$.

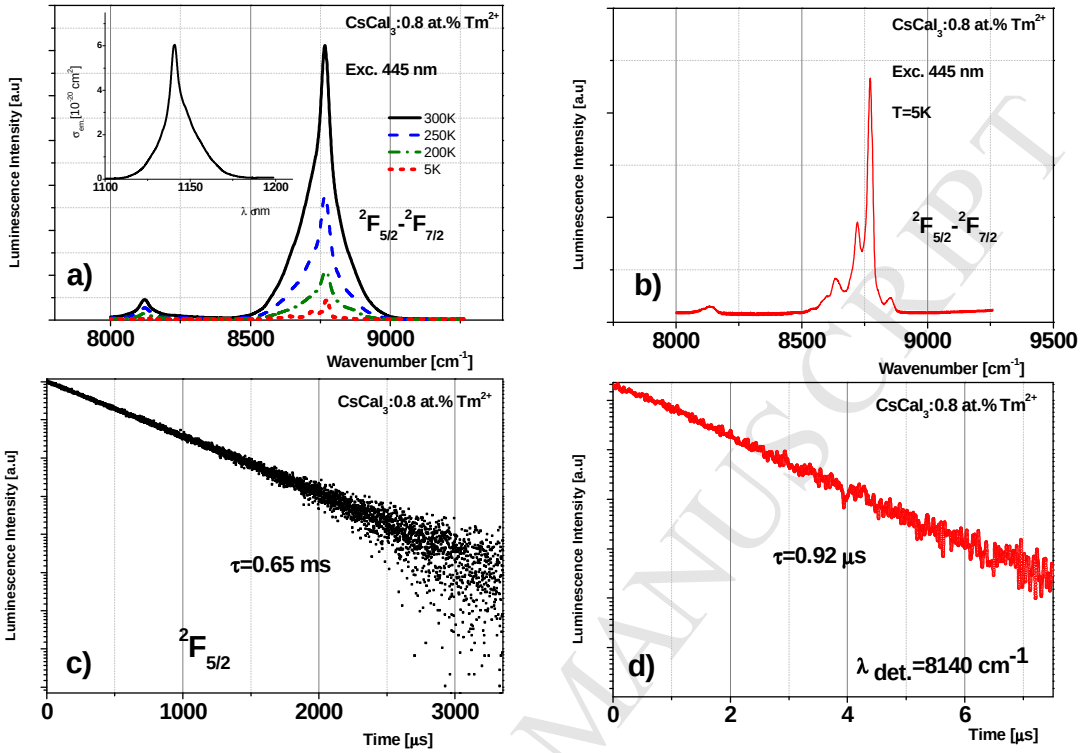

Fig. 2. a) Impact of temperature on $^2F_{5/2}$-$^2F_{7/2}$ Tm^{2+} emission spectra excited at 445 nm - inset shows the emission cross-section spectrum. b) Emission spectrum measured at T=5K. c) Decay curve of luminescence detected at λ=8767 cm^{-1}. d) Decay curve of luminescence detected at λ=8140 cm^{-1}.

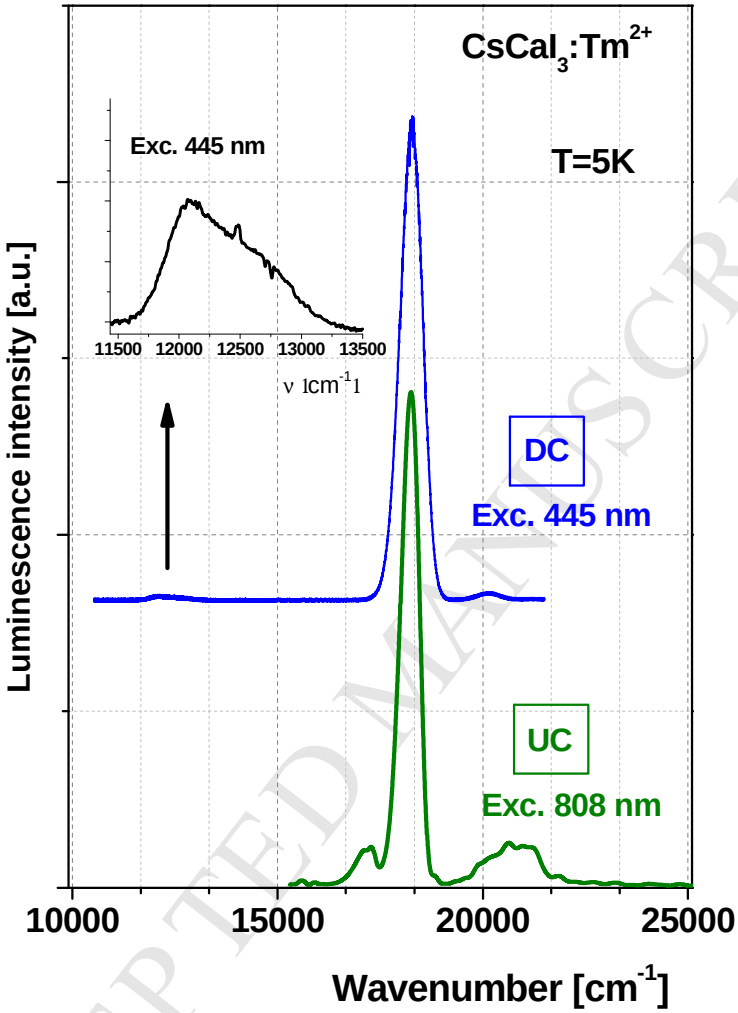

Fig. 3. Low-temperature (T=5K) emission spectra of $CsCaI_3$:0.68% Tm^{2+} crystal excited at 445 nm and 808 nm.

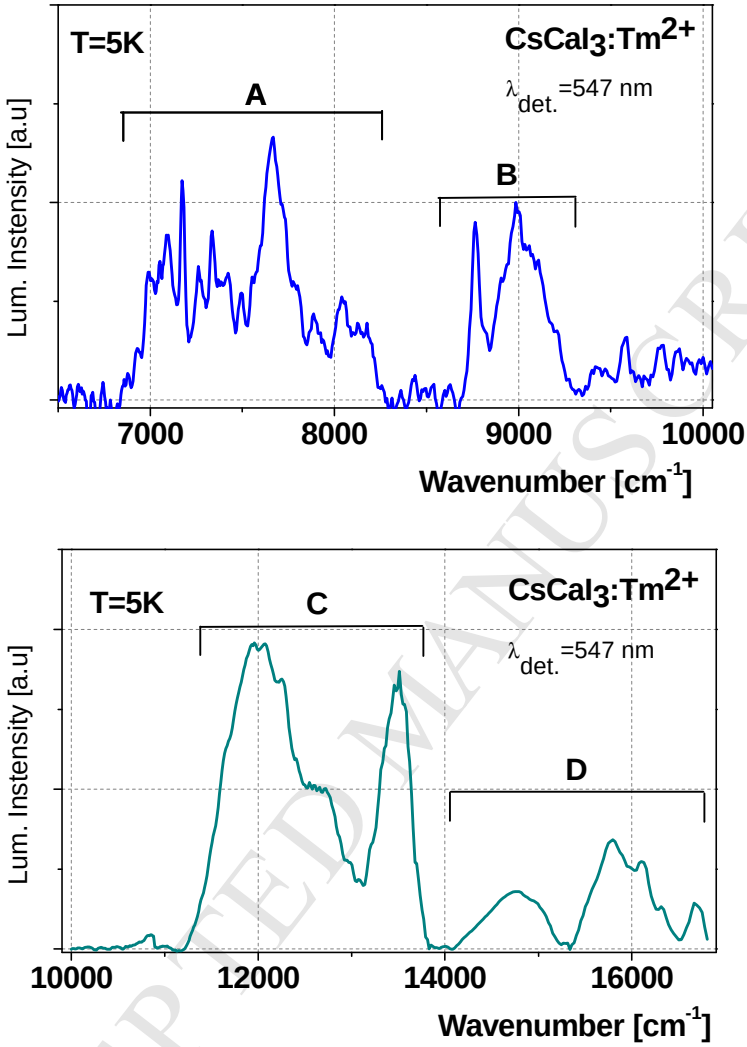

Fig. 4. Excited state excitation spectra of $CsCaI_3$:0.68% Tm^{2+} measured at T = 5K within 6000-17000 cm^{-1} spectral range. The luminescence was monitored at λ=547 nm.

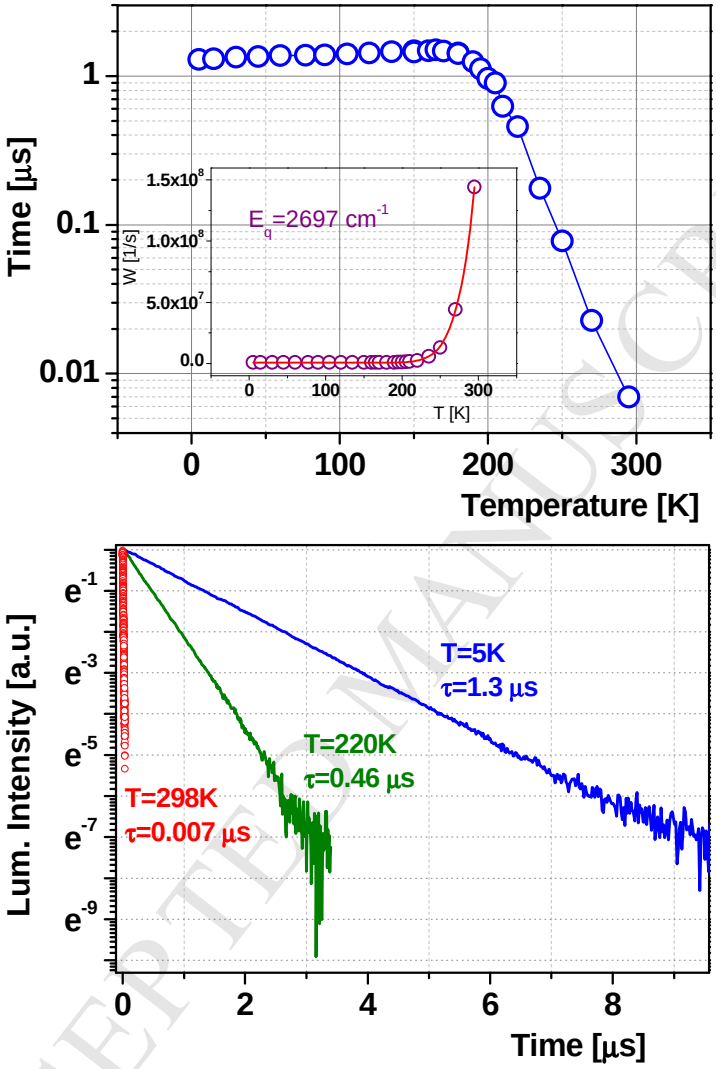

Fig. 5.Upper- Lifetime of the $CsCaI_3$:0.68% Tm^{2+} luminescence monitored at 18280 cm^{-1} and plotted versus temperature. The inset shows the activation energy E_g = 2697 cm^{-1} (± 15 cm^{-1}). Lower – Decay curves of thulium luminescence measured at different temperatures.

- Excited state excitation spectra are presented for Tm^{2+} in $CsCaI_3$.
- The $4f^{12}5d^1 \rightarrow 4f^{13}$ luminescence was analyzed in the function of temperature.
- Activation energy of $4f^{12}5d^1 \rightarrow 4f^{13}$ luminescence quenching was estimated.
- A high value of $^2F_{5/2} \rightarrow {}^2F_{7/2}$ emission cross-section was determined.